



Superhydrophilicity of anodic aluminum oxide films: From “honeycomb” to “bird's nest”

Jiaming Ye, Qiming Yin, Yongliang Zhou*

State Key Laboratory for Physical Chemistry of Solid Surfaces and Department of Chemistry, College of Chemistry and Chemical Engineering, Xiamen University, Xiamen 361005, P. R. China

ARTICLE INFO

Article history:

Received 25 April 2008

Received in revised form 14 April 2009

Accepted 17 April 2009

Available online 23 April 2009

Keywords:

Superhydrophilicity

Anodic aluminum oxide films

Structure-activity relationship

ABSTRACT

An electrochemical method has been used to prepare different kinds of surfaces including “honeycomb”-like and “bird's nest”-like surfaces on anodic aluminum oxide (AAO) films. The relationship between the morphology and wettability of the AAO films was investigated by scanning electron microscopy and the measurement of water contact angles. The results show that the “bird's nest”-like structure is necessary for superhydrophilic property, which provide direct experimental evidences for the 3D capillary theory concerning superhydrophilicity. It is expected that this investigation will be devoted to guiding the fabrication of superhydrophilic and superhydrophobic surfaces.

© 2009 Elsevier B.V. All rights reserved.

1. Introduction

Surfaces with special wettability, including superhydrophobic and superhydrophilic surfaces, have attracted significant interest in recent years, due to their wide practical applications ranging from self-cleaning surfaces to microfluidics [1–6]. Compared with the fabrication and the mechanism of superhydrophobic surfaces [7–11], the corresponding procedures concerning the superhydrophilic ones received much less attention [12–14], though they have similar potential in application.

The mechanism of superhydrophilicity was at first revealed by Wenzel [15], who discovered that roughening a surface enhanced its wetting properties. After 1997, based on studies of R. Wang et al. [16], the generation of superhydrophilicity on the surface of metal oxides contributed to hydrophilic nano-channels formed by photo-induced hydrophilic/hydrophobic domains, namely the “2D capillary effect”. In addition, Bico et al. proposed the “hemi-wicking” model or the “3D capillary effect” [17] to explain the superhydrophilicity of a textured surface by invasive behavior of water. However, very little reports have been put on the relationship between the geometrical structure and the superhydrophilicity of surfaces by experiments. Recently, by using micro electromechanical system or nano electromechanical system techniques, micro- and nano- pillar arrays have been fabricated to testify the above-mentioned theories [9,17]. In this paper, we used a single-step anodization method to fabricate different kinds of nano-structures on the anodic aluminum oxide (AAO) film including “honeycomb”-like and so-called “bird's nest”-like structures, by

adjusting electrochemical conditions such as the current density and the anodizing time. The relationship between the wettability and the nano-structure was investigated.

2. Experimental Section

2.1. Electrochemical fabrication

Aluminum foils (99.99% purity) with a thickness of 100 μm from Xinjiang JoinWorld Corporation were used as the starting material. All chemicals, unless otherwise specified, were obtained from the China National Pharmaceutical Group Corporation, and were analytically pure and used without further purification. Prior to anodizing, a piece of aluminum foil of 30 mm \times 40 mm size was degreased in acetone and immersed in a 1.0 M solution of NaOH until large numbers of hydric bubbles appeared on the surface of the aluminum plate, then thoroughly washed with deionized water. The treated aluminum plate was electropolished in a solution of 5 wt % phosphoric acid and glycerin (1:1 in volumetric ratio) at a constant voltage of 18 V for 30 min.

A single-step anodization procedure under a constant current mode was carried out in a 0.3 M solution of H_3PO_4 , using a two-electrode cell at 25 $^\circ\text{C}$. The aluminum plate was placed accurately right opposite to a platinum plate of the same size. The distance between the anodic aluminum plate and cathodic platinum plate was 12 mm. In order to dissipate the heat generated during anodization, the constant temperature of the electrolyte solution was achieved with magnetic stirring and a circular water bath system. After a period of anodization under a constant current density, the surface of the aluminum plate was rinsed with deionized water and dried in a stream of nitrogen, and then its water contact angle was measured. When the contact

* Corresponding author. Tel.: +86 592 2181583; fax: +86 592 2183047.
E-mail address: ylzhou@xmu.edu.cn (Y. Zhou).

angle was less than 5° , the superhydrophilic AAO film was prepared successfully.

2.2. Characterization

The surface morphology and the cross section of AAO films were observed with a scanning electron microscopy (SEM, LEO-1530, Germany) operated at 20 kV. The diameter of nanopores on AAO film was evaluated by analyzing the total pore area of each surface SEM image using Scion Image based on NIH image to ascertain the average area per pore, hence the average pore diameter. While the pore depth of nanopores on AAO film was determined by the cross-sectional SEM images. Surface area of rough AAO films was measured by a gas absorption analyzer (Micromeritics TRISTART 3000, USA). The wettability of the AAO film was characterized by the measurement of the water contact angle on its surface at 25°C , using a commercial contact angle meter (Dataphysics, OCA-20). For each contact angle reported, five readings from different parts of the film surface were averaged out.

3. Results and discussion

Controllable nano-structures can be produced on the surface of aluminum through anodic oxidation [18–20]. During the anodic oxidation, an ordered porous layer, namely the “honeycomb”-like structure (Fig. 1a–c), formed on the aluminum substrate after the formation of a barrier layer of oxide. As the anodizing time was prolonged, the pores became wider and wider while the cell walls became thinner and thinner. Then some nanopores broke into bigger pits, forming a “bird’s nest”-like structure (Fig. 1d).

To further study the morphologic transformation of the AAO films during anodization process, the pores diameter and depth of the AAO films were evaluated. As seen in Fig. 2, the growth process of the pores was divided into two different regimes by anodizing time. The first regime, which runs from 30 min to 90 min, displays diameter and depth of the pores increased linearly at 2.5 nm/min and 100 nm/min respectively. According to the earlier studies of AAO [18,20], formation and solution of alumina, occurring simultaneously, was in a dynamic balance during the anodization. In this regime, the solvent action of the cell walls played a leading role. Thus the pore diameter increased with the anodizing time. On the other hand, the increase of the pore depth attributed to the amount of oxide formed, which is a function of electric current and time according to Faraday’s law. In the second

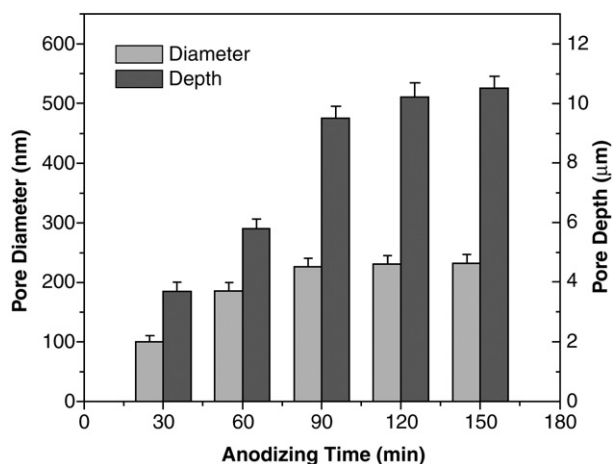


Fig. 2. Variation of dimension of the AAO nanopores with the anodizing time. The AAO films were prepared under an electric current density of 5 mA/cm^2 at 25°C .

regime, which begins at 90 min, diameter and depth of the pores remained constant, because the balance between oxide formation and solution was achieved.

It is noteworthy that after 90 min of anodizing, broken cell walls began to emerge on the surface of AAO. The amount of broken walls increased with the anodizing time, and then formed “bird’s nest”-like structures with interlaced sheets and wires in nano-scale (Fig. 3a). The size of a “bird’s nest” is around 1 to $2\ \mu\text{m}$, consisting of tens of broken sheets with a width of about 150 to 200 nm (Fig. 3b). Furthermore, we conclude from the SEM image of the cross section of the AAO film (Fig. 3c) that cell walls only break up on the surface of nanopores, and there are still regular nanopores beneath a “bird’s nest”.

The equilibrium water contact angle of the different AAO surfaces was examined. It was found that a flat aluminum surface after electropolishing showed a water contact angle of about 33° , while the honeycomb-like surface after 30 min anodizing showed about 26° , and then decreased to 17° after 60 min and 7° after 90 min. When the “bird’s nest”-like structure was formed on AAO films, the water contact angle on this surface declined to less than 3° and $1\ \mu\text{L}$ water spread and permeated quickly (around 0.8 s) when dropped on the surface (Fig. 3d), demonstrating the “bird’s nest”-like surface was indeed superhydrophilic. This indicates that the hydrophilicity of AAO

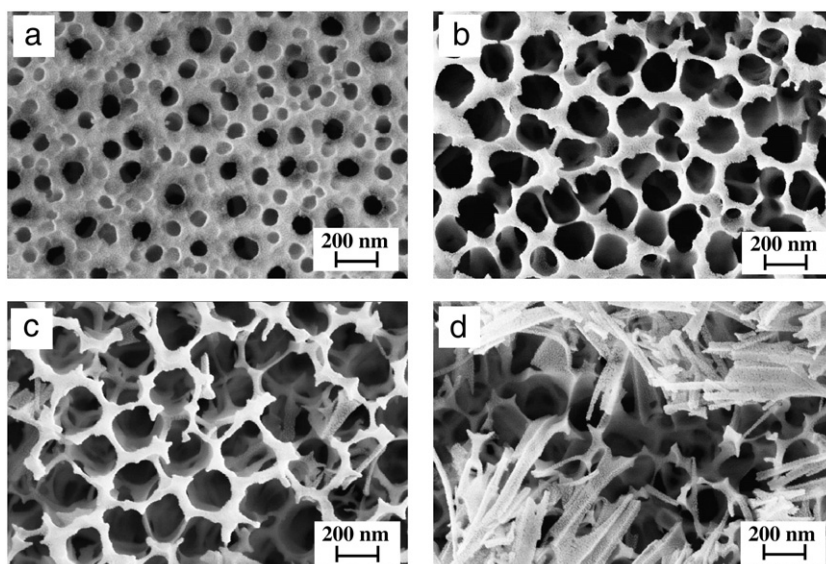


Fig. 1. SEM images of the porous AAO surfaces anodized in $0.3\text{ M H}_3\text{PO}_4$ for 30 min (a), 60 min (b), 90 min (c), and 120 min (d), under an electric current density of 5 mA/cm^2 at 25°C .

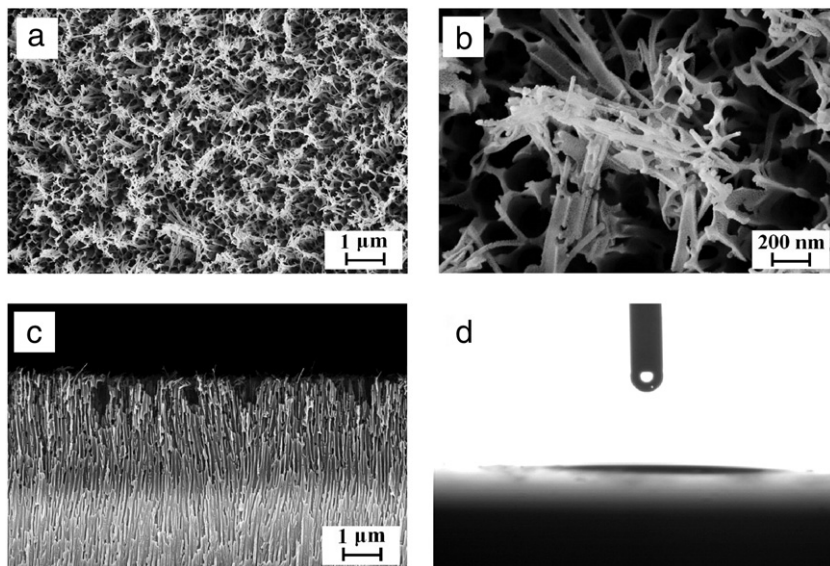


Fig. 3. SEM images of the superhydrophilic AAO film (a) view of the surface (lower magnification), (b) view of the surface (higher magnification), (c) cross sectional view, and (d) photograph of 1 μL water drop spreading on the relevant surface.

surfaces increases with the anodizing time. That is to say, the surface with wider and deeper pores is more hydrophilic, and only a “bird’s nest”-like surface presents superhydrophilicity.

According to Wenzel’s theory, the apparent contact angle θ_r of a liquid droplet placed on the rough solid surface is given by the following equation:

$$\cos\theta_r = r\cos\theta \quad (1)$$

where θ is the equilibrium contact angle of the liquid on an ideal flat surface of the same chemical composition, and r is a roughness factor, defined as the ratio of an actual rough surface area to the geometrically projected area. Assumed that the actual solid area of “honeycomb”-like surfaces equals the sum of the geometric projected area (S_p) and the total surface area of the side-walls (S_w), then the roughness factor r can be estimated by $r = (S_p + S_w) / S_p$. In our case, S_p is the given area for each SEM image of surface morphology, and S_w approximately equals to the product of the pore depth and the total pore perimeter depending on the pore diameter. For the “bird’s nest”-like surfaces, their actual solid area could not be calculated based on the above method due to the prominent irregularity of surface

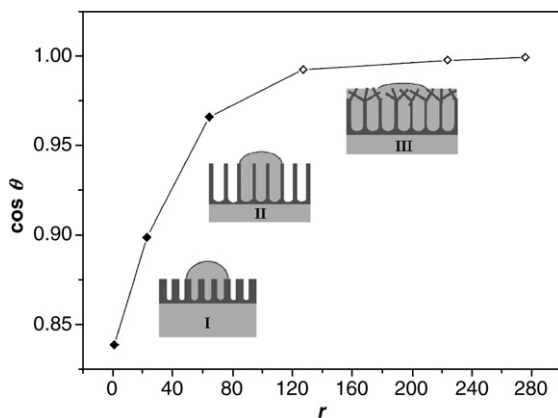


Fig. 4. Variation of the cosine of water contact angles with surface roughness factor for AAO films. Filled diamonds (◆) and empty diamonds (◇) correspond to the roughness factor estimated by SEM imaging and BET technique respectively. The inset I, II and III show the schematic transformation from hydrophilicity to superhydrophilicity of an AAO film.

structure, so we measured them by means of BET technique with a gas absorption analyzer. As is shown in Fig. 4, it is clear that in the case of “honeycomb”-like surfaces with a small r from 0 to 64, $\cos\theta_r$ is proportional to r which is in agreement with Wenzel’s theory (Eq. (1)). In other words, the surface with wider and deeper nanopores has a larger r , resulting in a larger $\cos\theta_r$, which means it is more hydrophilic. However, when the “honeycomb”-like structure was converted to the “bird’s nest”-like one, associated with an r larger than 127, the value of $\cos\theta_r$ has no significant differences with the increase of r due to the superhydrophilicity of AAO. The insets of Fig. 4 show the schematic drawings of the transformation from hydrophilicity to superhydrophilicity of an AAO film. As illustrated in the inset I, according to Wenzel’s model, when a water drop was placed on the “honeycomb-like” surface of an AAO film with a small r of about 23, no air was trapped in the nanopores under the droplet and the surface was dry

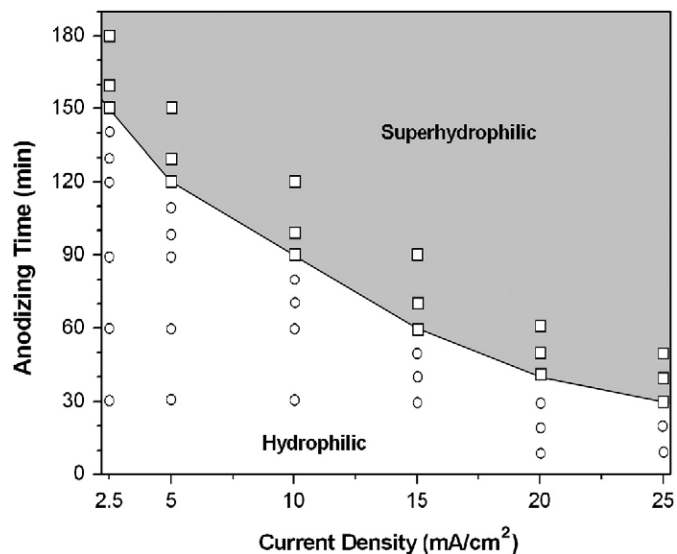


Fig. 5. The relationship between anodization current density and time for preparing superhydrophilic AAO surface. The square (□) data points and grey area represent parameters for preparing superhydrophilic surface, and the circle (○) data points and white area indicate that of hydrophilic surface respectively. The line between the grey and white areas denotes the minimum anodizing time for preparing superhydrophilic AAO surface under a certain current density.

ahead of the contact line. As the value of r increasing to about 65, Wenzel's model is still applicable, although the nanopores become deeper and wider (inset II in Fig. 4). When the “honeycomb”-like surfaces were converted to the “bird's nest”-like ones, $\cos \theta_r$ of which was close to 1 so that Wenzel's model was not suitable any more. The superhydrophilicity could be explained by the “3D capillary effect”. Due to the wicking and imbibition effect in the three-dimension capillary-structure consisting of broken sheets and nanopores, the water droplet would spread rapidly and a thin composite solid/liquid film was formed (inset III in Fig. 4), superhydrophilicity of the surface finally occurred.

Based on the above analysis, it is concluded that the “bird's nest”-like surface structure is crucial for a superhydrophilic AAO film. Generally, under a certain current density, the structural transformation from “honeycomb” to “bird's nest” on an AAO film surface could be realized by anodizing for enough time. In order to investigate the relationship between anodization current density and time for preparing superhydrophilic AAO surface, we measured the wettability of AAO films anodized with different time and current density, and found that the hydrophilicity of AAO films increased with increasing anodized time and the minimum time for preparing superhydrophilic AAO surface decreased with the increase of current density. As shown in Fig. 5, the line between grey and white areas denotes the minimum time for preparing superhydrophilic AAO surface under certain current density, and the grey area means parameters for preparing superhydrophilic surface. It can be observed clearly that the needed time for superhydrophilic AAO films declined with the increase of anodic current density. Therefore, by adjusting the anodic current density or anodizing time, superhydrophilic AAO films could be prepared effectively.

4. Conclusion

In summary, we have used an electrochemical method to prepare different kinds of surfaces including “honeycomb”-like and “bird's nest”-like surfaces on AAO films. The relationship between the morphology and wettability of the AAO films demonstrates that the

“bird's nest”-like structure is necessary for their superhydrophilic property. Our results offer direct experimental evidences for 3D capillary theory of superhydrophilicity proposed by Bico et al [17]. It is expected that this investigation will be helpful for guiding the fabrication of superhydrophilic surfaces.

Acknowledgements

The financial support of the National Science Foundation of China (20675066) and National Basic Research Program of China (973 Program, 2007 CB935603) is gratefully acknowledged. The authors also thank Prof. Lei Jiang and his research group for their helpful discussions and their assistance on the water CA measurements.

References

- [1] R. Blossey, *Nat. Mater.* 2 (2003) 301.
- [2] X.J. Feng, L. Jiang, *Adv. Mater.* 18 (2006) 3063.
- [3] P. Roach, N.J. Shirtcliffe, M.I. Newton, *Soft Matter* 4 (2008) 224.
- [4] R. Füstner, W. Barthlott, *Langmuir* 21 (2005) 956.
- [5] F.Ç. Cebeci, Z.Z. Wu, L. Zhai, R.E. Cohen, M.F. Rubner, *Langmuir* 22 (2006) 2856.
- [6] J.H. Zhang, X.F. Gao, L. Jiang, *Langmuir* 23 (2007) 3230.
- [7] T. Onda, S. Shibuichi, N. Satoh, K. Tsujii, *Langmuir* 12 (1996) 2125.
- [8] N.J. Shirtcliffe, G. McHale, M.I. Newton, G. Chabrol, C.C. Perry, *Adv. Mater.* 16 (2004) 1929.
- [9] E. Martines, K. Seunarine, H. Morgan, N. Gadegaard, C.D.W. Wilkinson, M.O. Riehle, *Nano. Lett.* 5 (2005) 2097.
- [10] L. Vogelaar, R.G.H. Lammertink, M. Wessling, *Langmuir* 22 (2006) 3125.
- [11] I.A. Larmour, S.E.J. Bell, G.C. Saunders, *Angew. Chem. Int. Ed.* 46 (2007) 1710.
- [12] T. Uelzen, J. Müller, *Thin Solid Films* 434 (2003) 311.
- [13] S. Permpoon, M. Houmar, D. Riassetto, L. Rapenne, G. Berthomé, B. Baroux, J.C. Joud, M. Langlet, *Thin Solid Films* 516 (2008) 957.
- [14] K.J. Tang, X.F. Wang, W.F. Yan, J.H. Yu, R.R. Xu, *J. Membr. Sci.* 286 (2006) 279.
- [15] R.N. Wenzel, *Ind. Eng. Chem.* 28 (1936) 988.
- [16] R. Wang, K. Hashimoto, A. Fujishima, M. Chikuni, E. Kojima, A. Kitamura, M. Shimohigoshi, T. Watanabe, *Adv. Mater.* 10 (1998) 135.
- [17] J. Bico, C. Tordeux, D. Quéré, *Europhys. Lett.* 55 (2001) 214.
- [18] H. Masuda, F. Hasegawa, *J. Electrochem. Soc.* 144 (1997) L127.
- [19] K. Tsujii, T. Yamamoto, T. Onda, S. Shibuichi, *Angew. Chem. Int. Ed. Engl.* 36 (1997) 1011.
- [20] A.I. Vorobyova, E.A. Outkina, *Thin Solid Films* 324 (1998) 1.